Alkane Transfer?Dehydrogenation Catalyzed by a Pincer-Ligated Iridium Complex

ARTICLE *in* CHEMINFORM · JANUARY 2005

Impact Factor: 0.74 · DOI: 10.1002/chin.200504269

4 AUTHORS, INCLUDING:

Alan S. Goldman
Rutgers, The State University of New Jersey
152 PUBLICATIONS **4,978** CITATIONS
SEE PROFILE

Karsten Krogh-Jespersen
Rutgers, The State University of New Jersey
183 PUBLICATIONS **5,375** CITATIONS
SEE PROFILE

ACS Symposium Series 885, *Activation and Functionalization of C-H Bonds,*
Karen I. Goldberg and Alan S. Goldman, eds. 2004.

Chapter 12

Alkane Transfer-Dehydrogenation Catalyzed by a Pincer-Ligated Iridium Complex

Alan S. Goldman, Kenton B. Renkema, Margaret Czerw, and Karsten Krogh–Jespersen

Department of Chemistry and Chemical Biology
Rutgers, The State University of New Jersey
New Brunswick, NJ 08903

The mechanism of (PCP)Ir-catalyzed transfer-dehydrogenation and a full free-energy profile have been elucidated for the substrate/acceptor couple COA/TBE (COA = cyclooctane; TBE = *t*-butylethylene). Stoichiometric components of the catalytic cycle have been independently observed and their kinetics have been determined. The overall catalysis has also been monitored *in situ*. Good agreement is found between rates independently obtained from stoichiometric and catalytic runs. Within the overall TBE-hydrogenation segment of the cycle, labeling experiments indicate that the rate-determining step is the C-H reductive elimination of *t*-butylethane from (PCP)IrH(*t*-butylethyl). Based on microscopic reversibility it can be then inferred that the rate-determining step for the alkane dehydrogenations is C-H addition (and not β-H elimination). In accord with this conclusion, *n*-alkanes are found to be more reactive than COA. A full energy profile for an *n*-alkane/α-olefin substrate/acceptor system can be extrapolated based on stoichiometric comparisons with the COA/TBE couple. A computed (DFT) free-energy profile generally matches well with the experimentally derived profile.

Olefins constitute the most important feedstock of the chemical industry. The dehydrogenation of alkanes is the most direct and potentially the most economical route to the production of olefins. While heterogeneous catalysts have long been used for the dehydrogenation of ethane and (less successfully) propane and isobutane (*1*), no such systems have been found capable of dehydrogenating higher alkanes to olefins with good chemoselectivity. In the early 1980's, Crabtree and Felkin developed homogeneous catalyst systems that used sacrificial hydrogen acceptors (*2*). These transfer-dehydrogenation systems showed excellent chemoselectivity but turnover numbers were limited by catalyst degradation. Systems developed subsequently have shown much higher turnover numbers and, in some cases, even high regioselectivity (*3*), but rates and conversions are still well below practical levels. Presently, the most effective such systems are those based upon pincer-ligated iridium (*4-6*), the first example of which was reported by Kaska and Jensen (*4a*). With cyclooctane/*t*-butylethylene (COA/TBE), the prototypical substrate/acceptor couple first introduced by Crabtree (*2*), it was found that (PCP)IrH_2 (**1;** PCP = 2,6-$C_6H_3(CH_2P^tBu_2)_2$) catalyzed transfer-dehydrogenation to give cyclooctene (COE) and 2,2-dimethylbutane (*t*-butylethane; TBA) with high rates and turnover numbers (*4a*).

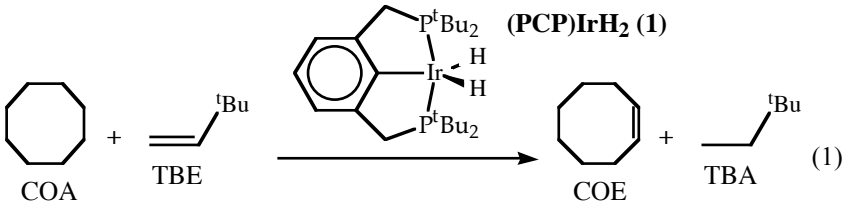

Herein, we report our elucidation of the mechanism of eq 1 (*7*). From this starting point we can extrapolate a full energy profile for a system in which *n*-alkane/α-olefin is the substrate/acceptor couple. The latter couple is not only of far greater potential utility (e.g. with propene as acceptor and long-chain *n*-alkane substrates), but it also presents the additional advantage of being far more amenable to computational modeling.

Stoichiometric Reactions with TBE and COA

In an effort to dissect the cycle of eq 1 into its component steps we first reacted the dihydride **1** with TBE in the absence of alkane. We thereby hoped to observe the hydrogenation segment of the cycle, which we presumed would include dehydrogenation and hydrogenation reactions.

In mesitylene (which appears to act as an inert solvent) **1** was found to react with two equiv TBE: one equiv TBE is hydrogenated and a second equiv

undergoes vinylic C-H addition to give (PCP)IrH(^{tBu}Vi) (**2**); ^{tBu}Vi = *trans*-2-[*t*-butyl]vinyl; eq 2) (*8*).

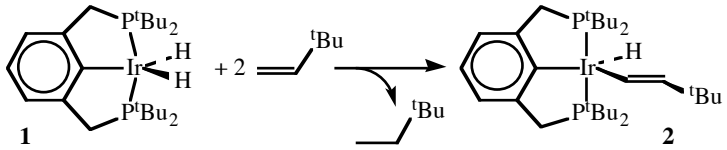

(2)

We had previously reported **2** and found that it undergoes rapid exchange with free TBE (on the NMR timescale) at ambient temperature via reversible loss of TBE (eq 3) (*9*).

(PCP)IrH(^{tBu}Vi) (**2**) ⇌ "(PCP)Ir" + TBE (3)

The kinetics of reaction 2 were studied by monitoring (^{1}H NMR) the disappearance of **1** and appearance of **2** at 55 °C in the presence of a slight excess of TBE. Both dependencies could be well fit with a single parameter, k_h = 0.57 M^{-1} min^{-1} where $-d[\mathbf{1}]/dt = d[\mathbf{2}]/dt = k_h[\mathbf{1}][TBE]$.

When COA is added to **2** (in *p*-xylene solvent at 55 °C) a rapid reaction ensues (eq 4).

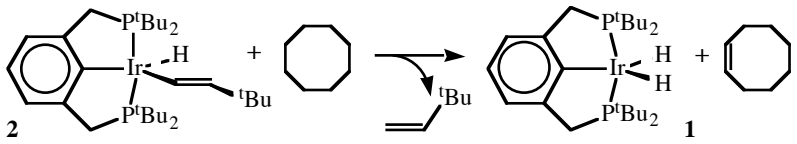

(4)

The sum of reactions 2 and 4 is the catalytic reaction 1. Thus, the two reactions constitute a possible mechanism for the catalytic transfer-dehydrogenation. However, before it could be concluded that the observed reactions constitute the major operative pathway, it remained to be determined if the catalytic and stoichiometric kinetics could be reconciled.

Unfortunately, whereas it was possible to isolate the suspected half of the catalytic cycle leading to TBE hydrogenation (eq 2) and then study its kinetics, the suspected second half of the cycle (eq 4) is too rapid to measure at 55 °C at low [TBE] (< ca. 0.2 M). Higher [TBE] inhibited reaction 4, but under such conditions reaction 2 then proceeds too rapidly to allow the independent measurement of the rate of reaction 4. Nevertheless, the observation of inhibition by added TBE suggests that the reaction proceeds via free "(PCP)Ir". This, in turn, suggests that the use of precursors of free (PCP)Ir other than **2** might permit study of COA dehydrogenation (as in 4) without the complications introduced by subsequent reaction of **1** with TBE.

We had previously reported a study of (PCP)IrH(Ph), an analogue of **2** (*9*). This complex was found to undergo dissociative hydrocarbon exchange in analogy with the behavior of **2** (eq 3). (PCP)IrH(Ph) could therefore in principle act as a "surrogate" source of (PCP)Ir, the intermediate that seemed likely to undergo the alkane C-H bond addition.

(PCP)IrH(Ph) undergoes reaction with COA (eq 5), in analogy with the reaction of **2** (eq 4).

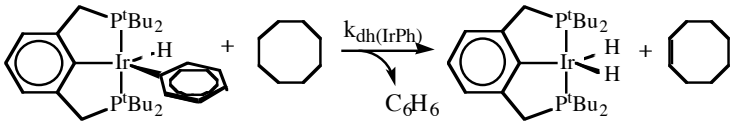

(5)

Disappearance of (PCP)IrH(Ph) and the increase of [(PCP)IrH$_2$] were monitored by ^{1}H NMR in the presence of an excess of benzene. The two resulting curves (Fig. 1) could be fit with a single parameter, $k_{dh(IrPh)}$, according to eq 6.

$$-d[(PCP)IrH(Ph)]/dt = d[\mathbf{1}]/dt = k_{dh(IrPh)}[(PCP)IrH(Ph)][COA][C_6H_6]^{-1} \qquad (6)$$

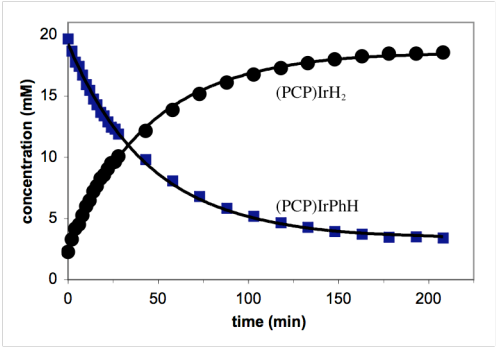

*Figure 1. Concentrations of [**1**] and [(PCP)IrH(Ph)] vs. time (eq 5)*

The value of $k_{dh(IrPh)}$ at 55 °C was determined to be 0.0023 min^{-1}. In order to extrapolate the analogous rate constant for the actual complex of interest (vinyl hydride, **2**) it is sufficient to only determine the equilibrium constant for eq 7.

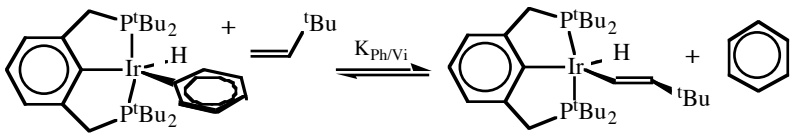

(7)

This extrapolation is valid assuming that the dehydrogenations of reactions 4 and 5 both proceed through a pre-equilibrium involving (PCP)Ir or through *any* other common intermediate. $K_{Ph/Vi}$ (eq 7) was found to equal 0.33. Applying this value to $k_{dh(IrPh)}$, we obtain a value of 0.0070 min^{-1} for k_{dh}, the analogous rate constant for the reaction of **2** with COA (eq 4).

Monitoring the Catalytic Reactions of TBE and COA *in situ*

The catalytic COA/TBE transfer-dehydrogenation was monitored directly (*in situ*) by ^{31}P NMR and by ^{1}H NMR (*7*). The only ^{31}P NMR-visible species present in significant concentrations were **1** and **2**.

Based on the mechanism of eqs 2 and 4 and the corresponding rate laws, the ratio of [**1**] to [**2**] can be predicted by considering the steady state of eq 8.

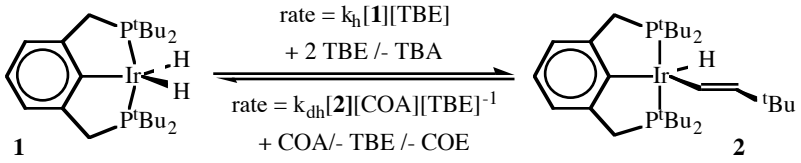

(8)

Thus, in the steady state, k_h[**1**][TBE] = k_{dh}[**2**][COA][TBE]$^{-1}$ which yields eq 9.

$$[\mathbf{2}]/[\mathbf{1}] = k_h[TBE]^2/k_{dh}[COA] \quad (9)$$

Figure 2 reveals that the measured concentrations are in excellent agreement with eq 9. The slope of the line in Figure 2 is equal to k_h/k_{dh}[COA], yielding $k_h/k_{dh} = 56\ M^{-1}$.

The catalytic turnover rate predicted by the mechanism of eqs 2 and 4 is simply equal to the rate of either of these two reactions under catalytic (steady-state) conditions (eq 10). Eq 9 can be re-written as eq 11; substitution into eq 10 then gives the full rate law, eq 12.

$$\text{rate} = d[COE]/dt = -d[TBE]/dt = k_h[\mathbf{1}][TBE] \quad (10)$$

$$[\mathbf{1}] = k_{dh}[Ir_{tot}][COA]/(k_{dh}[COA] + k_h[TBE]^2) \quad (11)$$

$$d[COE]/dt = k_h k_{dh}[TBE][COA][Ir_{tot}]/(k_{dh}[COA] + k_h[TBE]^2) \quad (12)$$

According to eq 12, in the limit of low [TBE] the catalytic rate is equal to k_h[TBE][Ir_{tot}] (first order in [TBE]), while in the limit of high [TBE] the rate should be $k_{dh}[TBE]^{-1}$[COA][Ir_{tot}], inverse first-order in [TBE]. Experimentally, catalytic rates were determined by *in situ* ^{1}H NMR measurement of the increase in [COE] at various initial concentrations of TBE. In accord with eq 12, the curve of rate vs. [TBE] reveals a maximum (at ca. 0.4 M TBE; Figure 3).

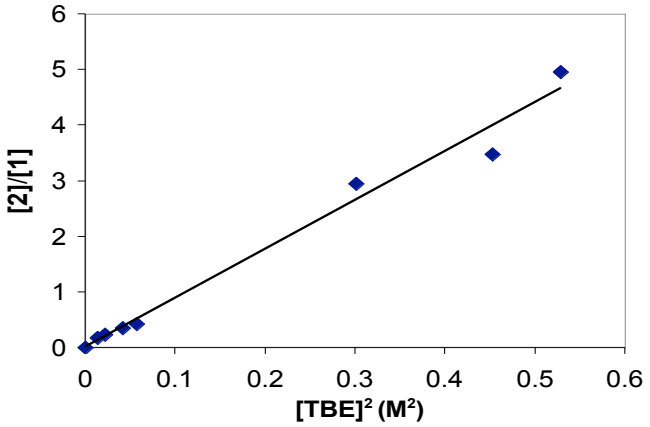

*Figure 2. Relative concentrations ([**2**] / [**1**]) vs. [TBE]^2*

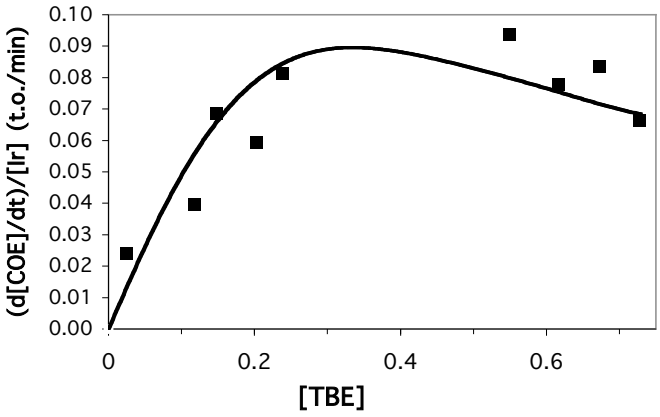

Figure 3. Rate of transfer-dehydrogenation (eq 1) vs. [TBE].

The curve shown in Figure 3 is calculated according to eq 12, generating a best fit to the data with k_h/k_{dh} held fixed at 56 M^{-1} (the value obtained from eq 9 and Figure 2). This therefore represents a one-parameter fit yielding the two rate constants, each obtained solely from *in situ* observation of the catalytic system: $k_h = 0.53\ M^{-1}\ min^{-1}$; $k_{dh} = 0.0094\ min^{-1}$.

The Full Catalytic Cycle: COA/TBE Transfer-Dehydrogenation

We now arrive at the critical question in the assessment of the proposed mechanism of eqs 2 and 4: Are the rate constants obtained from the stoichiometric experiments consistent with those obtained independently from the catalytic experiments? Considering experimental error and possible effects of different solvents (stoichiometric runs were necessarily conducted in non-alkane solvents, *p*-xylene or mesitylene) the agreement between the sets of rate constants is excellent (catalytic $k_h = 0.53\ M^{-1}\ min^{-1}$; $k_{dh} = 0.0094\ min^{-1}$; stoichiometric $k_h = 0.57\ M^{-1}\ min^{-1}$; $k_{dh} = 0.0070\ min^{-1}$). The overall set of kinetic equations is thus strongly overdetermined, and we consider these measured kinetics data to, effectively, prove the mechanisms of eqs 2 and 4 (Figure 4).

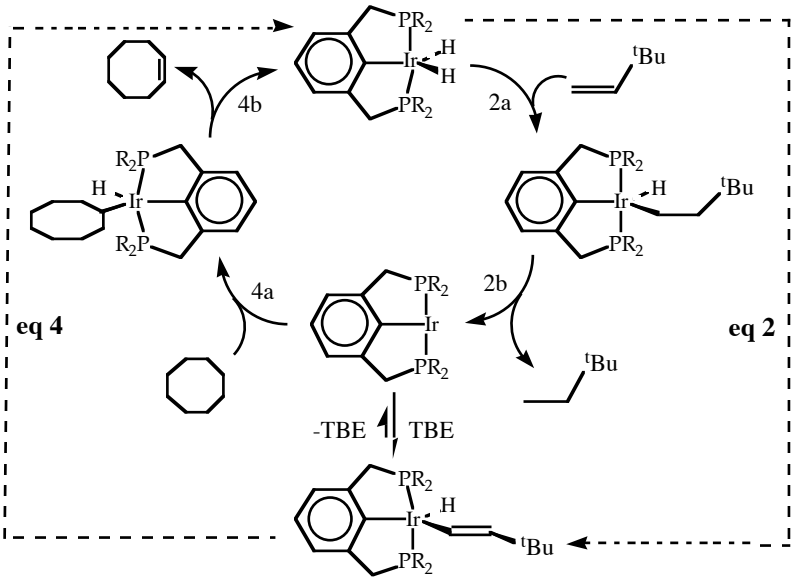

Figure 4. Mechanism of eq 1

Somewhat surprisingly, under typical conditions ([TBE] < ca. 0.3 M) the TBE-hydrogenation part of the cycle is rate-determining. We thus wished to

identify the rate-determining reaction step within the overall reaction 2. Toward this end, a labeling experiment was conducted to determine if the presumed insertion of TBE into the Ir-H bond is irreversible (i.e. if $k_{2b} >> k_{-2a}$, Figure 5).

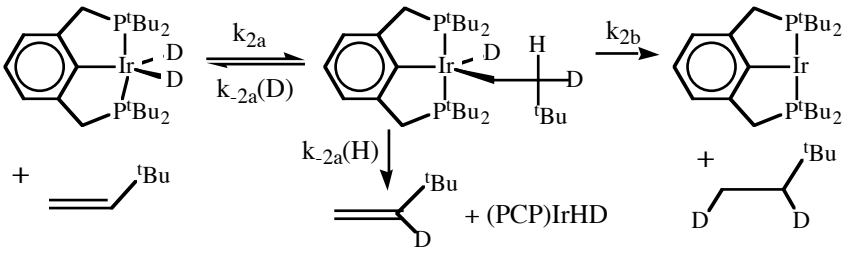

*Figure 5 . Reaction of **1** with TBE; competition between β-H (or β-D) elimination and C-H bond elimination*

(PCP-d_{36})IrD_2 (prepared via H/D exchange of **1** with C_6D_6) was reacted with TBE. The initial rate of formation of H/D exchanged product, CH_2=CD^tBu, was found to be 4.8 times greater than that of hydrogenated product, CH_2D-CHD(^{t}Bu). Neglecting isotope effects, we therefore obtain k_{-2a}/k_{2b} = 9.6, since statistically, formation of CH_2=CD^tBu should reflect half the rate of β-H elimination from the perproteo isotopomer.

The labeling experiment of Figure 5 demonstrates that the rate-determining step of reaction 2, and thus the rate-determining step of the catalytic cycle under typical conditions, is C-H elimination of TBA (2b, Figure 4). Based on considerations of microscopic reversibility, C-H *addition* must be the rate-determining step of the reverse reaction, the (hypothetical) *dehydrogenation* of TBA. This conclusion can be further extrapolated to the terminal dehydrogenation of *n*-alkanes (note that the lack of a bulky *t*-Bu group should facilitate β-H elimination more than C-H addition) and probably to cycloalkanes, which tend to undergo C-H addition less readily and β-H elimination more readily than *n*-alkanes (*10,11*). This finding presents an important contrast to previously reported alkane dehydrogenation systems, in which β-H elimination was found to be rate-determining (*2,3*).

A combination of several parameters can be used to determine a detailed full free-energy profile of the COA/TBE transfer-dehydrogenation cycle. These parameters include:

(1) rate constants k_h, k_{dh}

(2) rates of dissociation of TBE from (PCP)Ir(*t*-butylvinyl) (eq 3)

(3) relative reductive elimination/β-H elimination rates from the labeling experiment illustrated in Fig. 5 ($\Delta\Delta G^{\ddagger}$ = 1.5 kcal/mol, derived from the rate factor of 9.6)

(4) known thermodynamics of COA/TBE transfer-dehydrogenation (*12,13*)

In addition, we have determined the equilibrium constant (and thus ΔG) for eq 13 (*14*). Using $K_{Ph/Vi}$ (eq 7), K_{13} can then be used to determine the equilibrium constant and ΔG for the analogous reaction with **2** instead of (PCP)IrPhH (eq 14). This provides redundancy and an independent check on the relative thermodynamics of (PCP)IrH_2 and (PCP)IrH(*t*-butylvinyl) obtained from the parameters noted above.

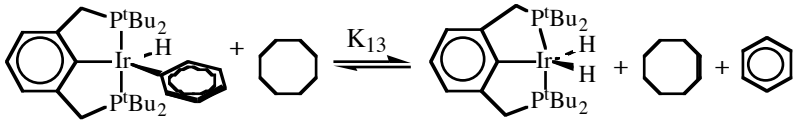

(13)

(PCP)Ir(H)(*t*-butylvinyl) + COA $\overset{K}{\rightleftharpoons}$ (PCP)IrH_2 + COE + TBE (14)

The rate constants (converted to free energies of activation) and equilibrium constants can be pieced together to give the free-energy profile shown in Fig. 6.

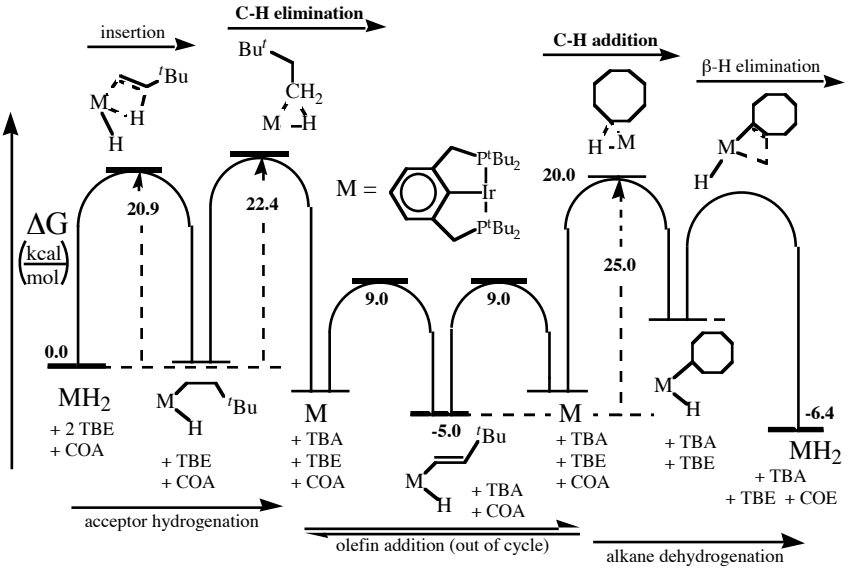

Figure 6. Free-energy profile for COA/TBE transfer-dehydrogenation cycle

Competition Experiment: COA vs. *n*-alkane

The results discussed above indicate that C-H addition is the rate-determining step in the dehydrogenation segment of the catalytic cycle. The selectivity of addition of C-H bonds to late metals has been well studied by several groups (*10,11*). To our knowledge, addition to late metals is, in all cases, more favorable for aliphatic primary C-H bonds than for secondary. The widespread use of COA as a "model" substrate for alkane dehydrogenation is attributable to the factors that engender the anomalously favorable thermodynamics of COA dehydrogenation; the same factors come into play in a β-H elimination transition state, but not in a transition state for C–H addition. Indeed Bergman has found that COA is less reactive toward C-H addition than cyclohexane (which in turn is less reactive than the terminal groups of *n*-alkanes) (*11*). These considerations raised important questions: Is the (PCP)Ir system more reactive toward *n*-alkanes than COA? And if so, is COA more easily dehydrogenated by other catalytic systems because β-H elimination is rate-determining in those systems?

An experiment was run in which (PCP)IrH_2 catalyzed the competitive transfer-dehydrogenation of COA and *n*-octane, using norbornene as acceptor. In accord with our inference that C-H oxidative addition is rate-determining, we found that the *n*-alkane was significantly more reactive (by a factor of 5.7 on a per mol basis, or 15 per C-H bond if it is assumed that addition occurs exclusively at the terminal position of *n*-octane).

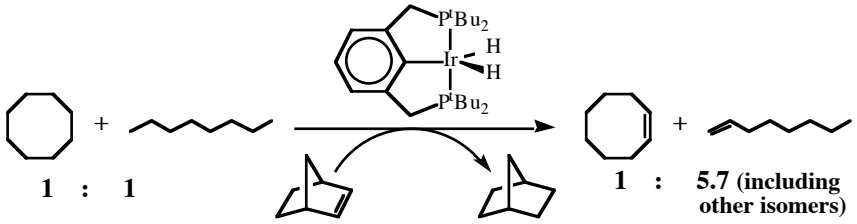

Figure 7 . Competition experiment: n-octane is more reactive than COA.

Inhibition of Catalysis Due to α-Olefin Binding

Despite the higher intrinsic reactivity of *n*-alkanes illustrated in Figure 7, preliminary results reveal that catalytic rates are generally comparable or somewhat faster for runs in which COA is the only dehydrogenation substrate as compared with *n*-alkane dehydrogenation. This apparent discrepancy can be easily rationalized in terms of a mechanistic scheme that is analogous to that shown in Figure 4. As indicated in Figure 4, the only resting states are **1** and the vinyl hydride, **2.** (COE can add to (PCP)Ir but much more weakly than either TBE or norbornene (*14*).) By contrast, in the case of dehydrogenation of *n*-alkanes, preliminary experiments reveal a different resting state: (PCP)Ir(η^2-1-

alkene). Thus, the relative *n*-alkane/COA rates in experiments with individual alkanes should depend strongly on conditions: in the regime where hydrogenation of acceptor is rate-determining, the nature of the substrate should have no effect. As the concentration of α-olefin increases in the *n*-alkane dehydrogenations, it will bind an increasingly large fraction of the iridium in solution and inhibit the reaction accordingly. The competition experiment of Figure 7, however, reveals the relative *intrinsic* reactivities of the two substrates.

The binding strength of α-olefin, relative to TBE C-H addition, was determined by equilibrium experiments, eq 15 (*14*).

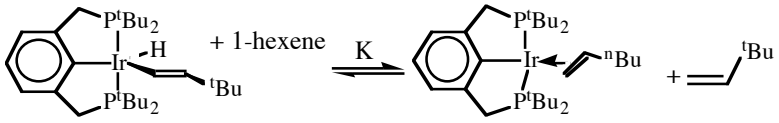

(15)

The relative rates of *n*-alkane/COA dehydrogenation and the relative α-olefin/TBE binding constants allow us to extrapolate a free-energy profile for *n*-alkane/α-olefin transfer-dehydrogenation. This extrapolation has several advantages: (i) the resulting profile describes (unlike COA/TBE) a potentially very useful system (e.g. formation of long-chain α-olefins using propene as an acceptor) (ii) the analysis is much simpler; because the reaction is degenerate, both halves are equivalent and the overall thermodynamics is obviously neutral (iii) for computational modeling there are fewer distinct intermediates and transition states due to the degeneracy, and they furthermore contain fewer atoms than either the analogous COA or TBE species (we use butane/butene as a model system). The resulting experimentally extrapolated free-energy half-profile (due to degeneracy the full profile is redundant) is shown in Figure 8.

Several points are worth noting in the context of Figure 8. *Vis-a-vis* the COA/TBE couple, *n*-alkane/α-olefin dehydrogenation is slowed by the strong binding of α-olefin (π-bonding) relative to TBE (C-H addition). The vinyl hydride species shown in Fig. 8 is never actually observed in this system; its energy is assumed to be approximately equal to the *t*-butylvinyl analog, although for steric reasons it might actually be lower. Crabtree's introduction of TBE as a hydrogen-acceptor seems particularly prescient in light of this diagram (*2*).

Figure 8 is in accord with preliminary observations that the ground state for *n*-alkane/α-olefin dehydrogenation is the π-bound α-olefin complex (*14*). However, the difference between this resting state and the dihydride is not necessarily the 7.0 kcal that might be inferred from Figure 8, since that value is based upon standard concentrations (1.0 M). Using typical concentrations the free-energy difference is substantially reduced. Further, the higher temperatures typically used for catalysis (values in Figure 8 are for 55 °C, the temperature of the mechanistic studies) favor the dihydride resting state (plus two mol free alkene) versus the vinyl hydride (plus one mol alkane) due to the entropic advantage of three free species versus two.

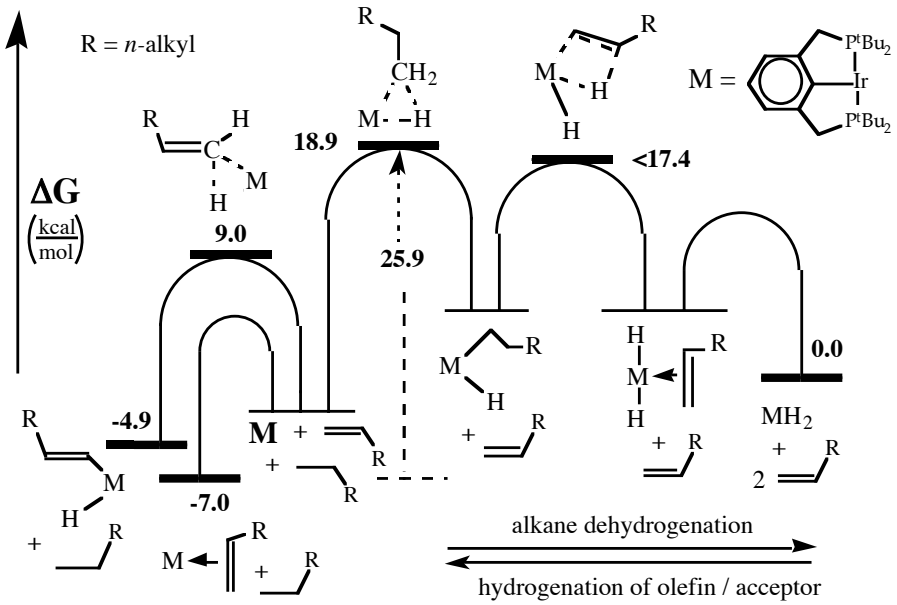

Figure 8 . Free-energy profile for n-alkane/α-olefin transfer-dehydrogenation cycle, experimentally extrapolated from COA/TBE profile.

DFT Calculations and Comparison of Theory with Experiment

We have conducted extensive computational (DFT) studies in parallel with our mechanistic work. We find that the theoretical results are far more valuable when viewed in the context of the experimental results rather than in isolation.

It is important to note that all calculated energies discussed herein are (Gibbs) free energies. The greatest differences between these and the purely electronic energies (E) arise from entropy terms. Entropy considerations are particularly important when comparing states of different molecularity; at 55 °C, such entropy differences can typically yield differences between electronic and free-energies of ca. 8 kcal/mol. In extreme cases (see the following Chapter in this Volume), the differences can be nearly 20 kcal/mol. Zero-point vibrational energy terms, which are also incorporated into the calculated free energies, can contribute several kcal/mol. Other factors tend to contribute less than these two terms (*15-17*).

It should also be noted that the work discussed herein utilizes alkyl groups (rather than H atoms) on the phosphorus ligands as should, in our opinion, all computational work where a *quantitative* comparison of theory and experiment is desired. Methyl groups serve as reasonably good models for *t*-butyl groups with respect to the purely electronic effects. However, they obviously do not capture the steric effects of *t*-butyl groups, and all computed results obtained with truncated ligands must therefore be carefully interpreted with this very important caveat in mind.

Calculations with ^{Me}PCP as Model Ligand

Figure 9 illustrates the free-energy profile for *n*-alkane/α-olefin transfer dehydrogenation predicted from DFT calculations using ^{Me}PCP as a model ligand (^{Me}PCP = 2,6-$C_6H_3(CH_2PMe_2)_2$; to distinguish this ligand from the analogous complex with *t*-Bu groups used experimentally, we will in this section specify the latter as $^{t\text{-}Bu}$PCP). The computed results are in overall good agreement with the experimentally derived profile, but only in a qualitative sense. Discrepancies encountered between experimental and calculated values are very much in accord with the reduced steric demands of Me (relative to *t*-Bu) groups. Using the free energy of the dihydride as the zero point, the calculated relative free energies of all species are lower than the experimentally established values by 4-10 kcal/mol with a single exception: (PCP)Ir(vinyl)H. This is a remarkably "sensible" result: the dihydride and vinyl hydride are probably the two species which encounter negligible steric crowding due to the small size of hydride ligands and the planarity of the vinyl group which enables the latter to fit unencumbered in the cleft of the ($^{t\text{–}Bu}$PCP)Ir equatorial plane. Note that addition/elimination of the vinyl C-H bond proceeds via a distinctly non-planar TS and is accordingly more crowded than the C–H addition product.

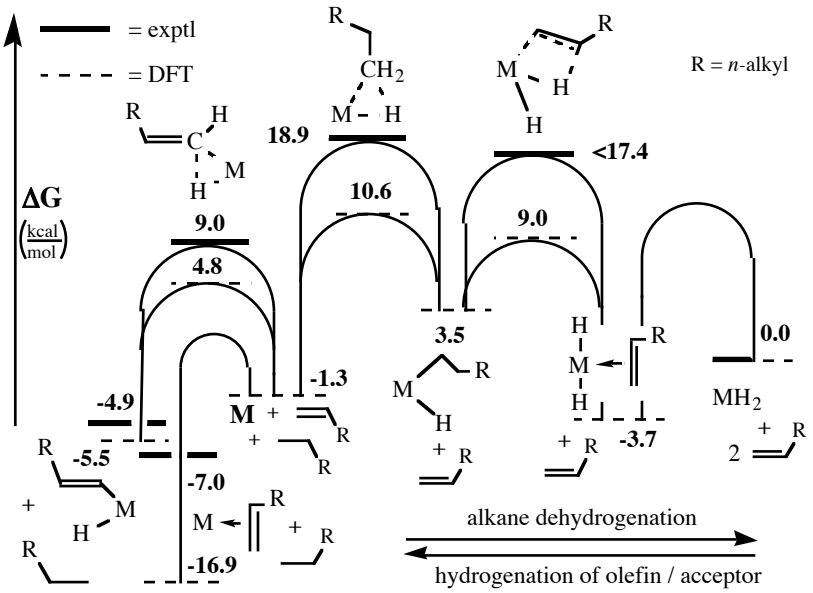

Figure 9. Free-energy profiles for n-alkane/α-olefin transfer-dehydrogenation (see Figure 8): experimental (M = (^{tBu}PCP)Ir) and DFT values (M = (^{tBu}PCP)Ir)

Of particular note is the calculated free-energy of the olefin dihydride complex, 3.7 kcal/mol below that of the dihydride. The actual olefin-dihydride species is undoubtedly of higher energy, since it never forms in observable concentration even though the actual catalytic pathway presumably proceeds through this state (in both directions). Since steric effects would be quite severe for this complex (with a $^{t\text{-}Bu}$PCP ligand), this discrepancy also makes good sense. Note that calculations ignoring entropy altogether and using the even less-bulky ^{H}PCP ligand (and C_2H_4 as model olefin) (*18*) suggest that loss of olefin from this complex would be the rate-determining step in the catalytic cycle. This suggestion is completely in discord with experimental observations, as would be expected in light of the above considerations. Using a similar approach, we obtain a relative free-energy value of –42 kcal/mol for the (PCP)Ir(olefin) complex, 49 kcal/mol less than the relative experimental free-energy!

Calculations with a Non-truncated Ligand: $^{t\text{-}Bu}$PCP

Calculations were also carried out using the full $^{t\text{-}Bu}$PCP ligand. However, due to the size of the molecular complexes involved, these calculations

necessarily employed a more limited basis set on the phosphine alkyl groups than the one used in the ^{Me}PCP calculations described above.

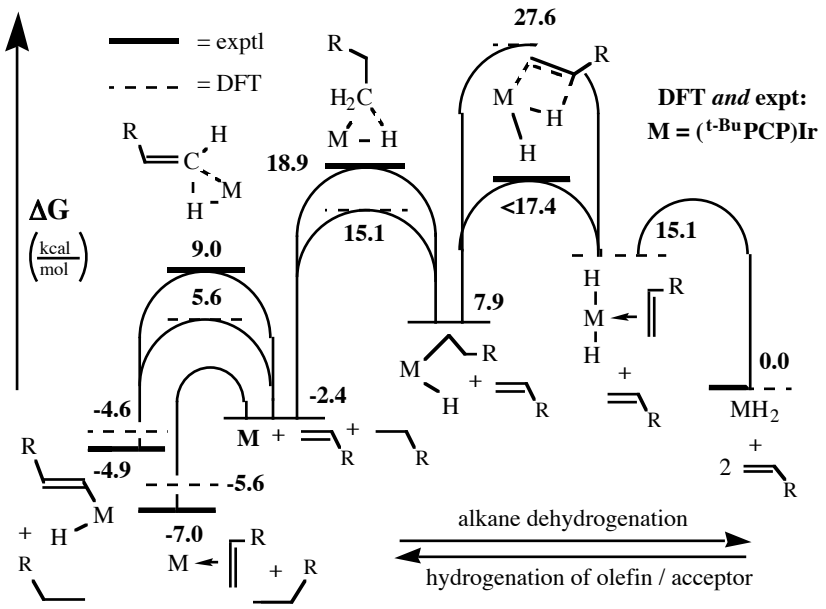

Figure 10. Free-energy profiles for n-alkane/α-olefin transfer-dehydrogenation (see Figure 8): experimental and DFT values for M = ($^{t\text{-}Bu}$PCP)Ir

The values obtained with the non-truncated $^{t\text{-}Bu}$PCP ligand were found to be in generally much better agreement with experiment (within 4 kcal/mol) than those calculated with ^{Me}PCP. The singular exception to this generalization is the TS for β-H elimination/olefin-insertion. This very crowded TS is calculated to be much higher in energy using ($^{t\text{-}Bu}$PCP)Ir than (^{Me}PCP)Ir, and the calculated free energy is significantly higher (~ 10 kcal/mol or more) than the experimental value. The high calculated value of the $^{t\text{-}Bu}$PCP TS for β-H elimination may be attributable to the pronounced tendency of DFT to overestimate steric interactions, since dispersion interactions are not included in the (B3LYP) functionals used in the calculations. Alternatively, H-atom tunneling may be contributing to an apparent reduction in the experimentally measured barrier.

Although these results illustrate some of the perils of taking at face value even the results of high-level free-energy calculations on non-truncated systems, we feel that they do also strongly suggest that DFT calculations can be of considerable value in predicting catalytic activity and catalyst design – provided the calculations are interpreted with due care. Although computational results of

"chemical accuracy" are not yet obtainable, precision within ca. 4 kcal/mol is certainly of great potential value for purposes of *in silico* catalyst "screening". And while the discrepancy found for the β-H elimination TS is serious, we believe it will be mostly reproducible with other complexes of $^{t\text{-}Bu}$PCP and sterically similar ligands. Thus, to a first approximation, we can apply this derived "calibration" to future calculations on related complexes and we are, in fact, currently screening a range of pincer complexes using this approach (*19*). We are also attempting to improve the precision of our calculations via the use of mixed-mode QM/MM methodologies and different functionals.

Summary

The mechanism of (PCP)Ir-catalyzed transfer-dehydrogenation of the COA/TBE substrate/acceptor couple has been elucidated and a detailed free-energy profile has been determined. The two segments of the cycle have been observed independently, and the nature of the rate-determining step within each segment has been determined. The mechanism has several notable features:

(i) Although olefin hydrogenation is one of the most widely and readily catalyzed reactions of organometallic complexes (*11*), the rate-determining (slow) segment of the present cycle under typical conditions is hydrogenation of TBE.

(ii) Although C–H addition is often assumed to be the "difficult" step in alkane functionalizations (*10*), in this case C-H *elimination* of alkane (TBA) is apparently rate-determining.

(iii) In the regime where dehydrogenation is the rate-determining segment (very high [TBE]), C-H addition is inferred to be the rate-determining step. Nevertheless, a substantial contribution to the overall barrier derives from the thermodynamic cost of eliminating the vinyl C-H bond of TBE prior to addition of the alkane C-H bond.

Consistent with the conclusion that C-H addition is rate-determining, *n*–alkanes are found to be intrinsically more reactive than COA (generally regarded as an "easily dehydrogenated" substrate). However, this is offset by the fact that the α-olefin dehydrogenation products bind more strongly than COE and thereby inhibit catalysis more severely. The *n*-alkane /COA and α-olefin/COE competition experiments allow us to extrapolate a full energy profile for *n*-alkane /α-olefin transfer-dehydrogenation.

DFT calculations of free energies show qualitative agreement with experimental results, when ^{Me}PCP models the experimentally used $^{t\text{-}Bu}$PCP ligand. However, the energetic and structural effects of the reduced crowding exerted by methyl groups are apparent. When calculations are conducted with the non-truncated $^{t\text{-}Bu}$PCP ligand, the agreement is generally much better. The energy of the TS for β-H elimination/olefin insertion is understated for ^{Me}PCP but significantly overstated using the full $^{t\text{-}Bu}$PCP ligand. The reasons for this discrepancy remain under investigation. In the interim, we believe it is possible

to use the experimental and computational values obtained in this work to "calibrate" the results of DFT calculations on related, sterically similar, systems for the purpose of computational catalyst screening.

Acknowledgement

We thank the Division of Chemical Sciences, Office of Basic Energy Sciences, Office of Energy Research and the U. S. Department of Energy for support of this research.

References

1. (a) Sundarum, K. M.; Shreehan, M. M.; Olszewski, E. F. In *Kirk-Othmer Encyclopedia of Chemical Technology*; 4th ed.; Kroschwitz, J. I., Howe-Grant, M., Eds.; Wiley-Interscience: New York, 1991; Vol. 9, pp 877-915. (b) Tullo, A. H. In *Chem. Eng. News*, 2001; Vol. 79, pp 18-24. (c) Goldman, A. S. In *Encyclopedia of Catalysis*; Horvath, I., Ed.; John Wiley & Sons, 2002; Vol. 3, pp 25-33.
2. (a) Crabtree, R. H.; Mihelcic, J. M.; Quirk, J. M. *J. Am. Chem. Soc.* **1979**, *101*, 7738. (b) Crabtree, R. H.; Mellea, M. F.; Mihelcic, J. M.; Quirk, J. M. *J. Am. Chem. Soc.* **1982**, *104*, 107. (c) Baudry, D.; Ephritikine, M.; Felkin, H. *J. Chem. Soc., Chem. Commun.* **1980**, 1243–1244. (d) Baudry, D.; Ephritikine, M.; Felkin, H.; Holmes-Smith, R. *J. Chem. Soc., Chem. Commun.* **1983**, 788. (e) Burk, M. J.; Crabtree, R. H.; Parnell, C. P.; Uriarte, R. J. *Organometallics* **1984**, *3*, 816.
3. (a) Maguire, J. A.; Goldman, A. S. *J. Am. Chem. Soc.* **1991**, *113*, 6706. (b) Maguire, J. A.; Petrillo, A.; Goldman, A. S. *J. Am. Chem. Soc.* **1992**, *114*, 9492.
4. (a) Gupta, M.; Hagen, C.; Flesher, R. J.; Kaska, W. C.; Jensen, C. M. *Chem. Commun.* **1996**, 2083. (b) Gupta, M.; Hagen, C.; Kaska, W. C.; Cramer, R. E.; Jensen, C. M. *J. Am. Chem. Soc.* **1997**, *119*, 840. (c) Gupta, M.; Kaska, W. C.; Jensen, C. M. *Chem. Commun.* **1997**, 461.
5. (a) Xu, W.; Rosini, G. P.; Gupta, M.; Jensen, C. M.; Kaska, W. C.; Krogh-Jespersen, K.; Goldman, A. S. *Chem. Commun.* **1997**, 2273. (b) Liu, F.; Goldman, A. S. *Chem. Comm.* **1999**, 655.
6. Liu, F.; Pak, E. B.; Singh, B.; Jensen, C. M.; Goldman, A. S. *J. Am. Chem. Soc.* **1999**, *121*, 4086.
7. Renkema, K. B.; Kissin, Y. V.; Goldman, A. S. *J. Am. Chem. Soc.* **2003**, *125*, 7770.
8. For closely related examples of oxidative addition of vinylic C-H bonds see: Wick, D. D.; Jones, W. D. *Organometallics* **1999**, *18*, 495.
9. Kanzelberger, M.; Singh, B.; Czerw, M.; Krogh-Jespersen, K.; Goldman, A. S. *J. Am. Chem. Soc.* **2000**, *122*, 11017.

10. For some reviews of alkane C-H bond activation by organometallic complexes see: (a) Arndtsen, B. A.; Bergman, R. G.; Mobley, T. A.; Peterson, T. H. *Acc. Chem. Res.* **1995**, *28*, 154. (b) Shilov, A. E.; Shul'pin, G. B. *Chem. Rev.* **1997**, *97*, 2879. (c) Sen, A. *Acc. Chem. Res.* **1998**, *31*, 550. (d) Guari, Y.; Sabo-Etiennne, S.; Chaudret, B. *Eur. J. Inorg. Chem.* **1999**, 1047. (e) Jones, W. D. *Science* **2000**, *287*, 1942. (f) Crabtree, R. H. *Journal of the Chemical Society, Dalton Transactions* **2001**, *17*, 2437. (g) Labinger, J. A.; Bercaw, J. E. *Nature* **2002**, *417*, 507-514.
11. See reference 10; other papers that have addressed selectivity in particular, and provide good lead references, include: (a) Harper, T. G. P.; Desrosiers, P. J.; Flood, T. C. *Organometallics* **1990**, *9*, 2523. (b) Bennett, J. L.; Vaid, T. P.; Wolczanski, P. T. *Inorg. Chim. Acta.* **1998**, *270(1-2)*, 414. (c) Wick, D. D.; Jones, W. D. *Organometallics* **1999**, *18*, 495. (d) Asbury, J. B.; Hang, K.; Yeston, J. S.; Cordaro, J. G.; Bergman, R. G.; Lian, T. *J. Am. Chem. Soc.* **2000**, *122*, 12870 and references 4-11 therein. (e) Peterson, T. H.; Golden, J. T.; Bergman, R. G. *J. Am. Chem. Soc.* **2001**, *123*, 455.
12. NIST Standard Reference Database Number 69 - March, 2003 Release: http://webbook.nist.gov/chemistry/
13. Enthalpy values of -30.1 and -24.3 kcal/mol are used for hydrogenation of COE and TBE respectively (liquid phase; ref 12); thus $\Delta H° = -5.8$ kcal/mol for the transfer-dehydrogenation. Based on respective entropy values (gas-phase value are used; ref 12) $\Delta S° = +1.77$ eu; giving $\Delta G° = -6.4$ kcal/mol at 55 °C.
14. Renkema, K. B.; Goldman, A. S., to be submitted for publication.
15. (a) Abu-Hasanayn, F.; Goldman, A. S.; Krogh-Jespersen, K. *J. Phys. Chem.* **1993**, *97*, 5890. (b) Abu-Hasanayn, F.; Krogh-Jespersen, K.; Goldman, A. S. *J. Am. Chem. Soc.* **1993**, *115*, 8019.
16. (a) Schaller, C. P.; Cummins, C. C.; Wolczanski, P. T. *J. Am. Chem. Soc.* **1996**, *118*, 591. (b) Slaughter, L. M.; Wolczanski, P. T.; Klinckman, T. R.; Cundari, T. R. *J. Am. Chem. Soc.* **2000**, *122*, 7953.
17. (a) Churchill, D. G.; Janak, K. E.; Wittenberg, J. S.; Parkin, G. *J. Am. Chem. Soc.* **2003**, *125*, 1403. (b) Janak, K. E.; Parkin, G. *J. Am. Chem. Soc.* **2003**, *125*, 6889.
18. Niu, S. Q.; Hall, M. B. *J. Am. Chem. Soc.* **1999**, *121*, 3992.
19. Achord, P.; Goldman, A. S.; Krogh-Jespersen, K., to be submitted for publication.